doi.org/10.36721/PJPS.2026.39.8.213.1

Quinazoline alleviates inner ear damage by enhancing the proliferation and differentiation of neural stem cells

Qinxue Wang[1]* and Yin Wang[2]
[1]Department of Otolaryngology, Shanxi Children's Hospital, Shanxi Maternal and Child Health Hospital, Taiyuan, Shanxi, 030600, China
[2]Department of Otolaryngology, Shanxi Children's Hospital, Taiyuan, Shanxi, 030600, China

Abstract: **Background**: Neural stem cell (NSC) transplantation exerts therapeutic effects on inner ear damage and pretreatment with quinazoline compounds may further enhance this efficacy. **Objectives**: This study aimed to investigate whether quinazoline alleviates inner ear damage by enhancing the proliferation and differentiation of NSCs. **Methods**: Forty Hartley guinea pigs were randomly assigned to four groups. Hippocampal NSCs isolated from neonatal guinea pigs were pretreated with quinazoline and transplanted into animals with cisplatin-induced hearing loss. Evaluations included NSC proliferation and differentiation, auditory brainstem response (ABR) thresholds and miR-183 expression in cochlear tissues. **Results**: Quinazoline pretreatment significantly enhanced NSC proliferation and differentiation ($P<0.05$). After transplantation, the group receiving quinazoline-pretreated NSCs showed a significantly lower ABR threshold (reflecting an approximately 10 dB improvement in hearing recovery) than the group receiving untreated NSCs ($P<0.05$). This was accompanied by more pronounced structural repair of the cochlea and a significant upregulation of miR-183 expression ($P<0.05$). **Conclusion**: Quinazoline promotes the repair of inner ear injury by enhancing the proliferation and differentiation of NSCs, a mechanism that appears to be associated with the upregulation of miR-183 expression.

Keywords: ABR threshold; Inner ear damage; miR-183; Mechanism; Neural stem cell; Proliferation and differentiation; Quinazoline

Submitted on 15-08-2025 – Revised on 29-12-2025 – Accepted on 15-01-2026

INTRODUCTION

Inner ear hearing loss, which can result from factors such as aging, ototoxic drugs and noise exposure (Duran Alonso, 2026), is a significant health concern. In China, the affected population has reached 20 million (Li *et al*., 2022), making the treatment of hearing loss a major research focus. Neural stem cells (NSCs) possess the defining characteristics of self-renewal and multi-lineage differentiation (Chao *et al*., 2021, Chen *et al*., 2021, Cui *et al*., 2021). Recent studies have shown that NSCs can differentiate into cell types relevant to the inner ear, such as hair cells and Schwann cells, offering therapeutic potential for hearing restoration (Dong *et al*., 2021; Dray *et al*., 2021; Diener and Sommer, 2021). Supporting this, transplantation of differentiated NSC-derived cells has been shown to improve auditory function in animal models (Gastfriend *et al*., 2021; Gao *et al*., 2021).

Therefore, researchers have proposed that exogenous and endogenous factors can influence NSC proliferation and differentiation. Targeting these factors may manipulate these processes and thereby ameliorate inner ear damage (Haag *et al*., 2021; Han *et al*., 2021; Gong *et al*., 2021). The endogenous factors mainly include nerve growth factors (epidermal growth factor (EGF), insulin-like growth factor (IGF), etc.) and hormones, while the exogenous factors mainly include compounds, nutrients, etc. (Hayashi *et al*., 2021; Hirai *et al*., 2021). Early predictions suggested that quinazoline could enhance NSC function (Huang *et al*., 2021) and a 2021 patent report formally proposed the use of quinazoline derivatives to regulate NSC proliferation and differentiation for neural repair applications (Jia *et al*., 2021). This finding invigorated research into cell replacement therapy for neurological conditions. Quinazolines are a class of compounds known for their ability to inhibit multiple growth factor receptors, conferring a range of biological activities. Their structural versatility and broad pharmacological profile have generated significant scientific interest. They have been successfully developed and used for commercial products, which include the fungicide fluquinazole, the acaricide drug fenazaquin and the anti-cancer drug Iressa.

Neural stem cell transplantation is a widely accepted therapy in clinical research and is employed for treating spinal cord damage, nervous system diseases, etc. Nevertheless, whether the compound-treated neural stem cells can exhibit the same or even more beneficial therapeutic effects requires further exploration. Currently, there are few studies focusing on the compound-treated neural stem cells with enhanced differentiation and proliferation capabilities used in managing neurodegenerative diseases. By studying the cochlear tissue condition and hearing threshold, our study aims to investigate whether quinazoline can alleviate inner ear damage by enhancing the differentiation and proliferation of neural stem cells.

**Corresponding author:* e-mail: 13593159463@163.com

MATERIALS AND METHODS

Experimental equipment and reagents

Phosphate-buffered saline(PBS) solution (Thermo Fisher Scientific); Quinazoline compound (Shanghai Fortune Biotech); Cell Counting Kit-8(CCK-8) reagent, 5-Ethynyl-2'-deoxyuridine (Edu) reagent, 4',6-Diamidino-2-phenylindole (DAPI), Neuron-specific enolase (NSE), Glial fibrillary acidic protein (GFAP, Beijing Think-far Technology); Auditory brainstem response instrument (Beijing Gemeishengda); Ethylenediaminetetraacetic acid (EDTA) solution, Hematoxylin and eosin (HE) solution (Thermo Fisher Scientific); Primers of miR-183 and β-actin (HePeng (Shanghai) Biotech).

Experimental animals

This study utilized 40 healthy Hartley strain guinea pigs (250-300g, equal numbers of male and female animals) with sensitive Preyer's reflex. All animals were randomly divided into four groups: control group, model group, transplantation group and enhancement group (10 guinea pigs per group). Guinea pigs in the control group received normal feeding without special treatment. Those in the model group received cisplatin to induce hearing loss. After the model was established, the guinea pigs in the transplantation group received neural stem cell transplantation (1×10^5/L), while those in the enhancement group received neural stem cell transplantation (1×10^5/L) and were treated with quinazoline (40 μg/mL), which exhibited significantly enhanced differentiation and proliferation capabilities. All the selected guinea pigs had no history of ototoxic drug use. Animals were raised under standard conditions (temperature 22±2°C, humidity 50±10%, 12-hour light/dark cycle) and are free to eat and drink.

Ten of the newborn guinea pigs (24-hour old) were selected and received normal feeding.

Animal source and housing: All guinea pigs were purchased from Beijing Vital River Laboratory Animal Technology Co., Ltd., Beijing, China. Animals were housed in groups of 2-3 per cage in standard polycarbonate cages (dimensions: 40 × 25 × 20 cm) with corncob bedding and environmental enrichment (PVC hiding tubes). Body weight, behavior, and food/water intake were monitored daily. Humane endpoints were defined as >20% body weight loss from baseline, inability to eat or drink spontaneously, or a moribund state. No animals reached humane endpoints or died during the study.

Randomization and blinding: Animals were randomly assigned to four groups (control, model, transplantation, and enhancement) using an Excel random number generator. ABR threshold measurements, morphological observation of cochlear tissues by HE staining, qPCR analysis, and data analysis were performed by investigators who were blinded to group allocation.

Sample size determination: Based on pilot study results (effect size = 1.2, $\alpha = 0.05$, power = 0.8), a sample size of 10 animals per group (total 40 animals) was calculated using PASS software.

Inclusion and exclusion criteria: Inclusion criteria were a sensitive Preyer's reflex and no history of ototoxic drug use. Exclusion criteria were an increase in ABR threshold of <30 dB from baseline after modeling (indicating failed model establishment), intraoperative death, or postoperative infection. No animals were excluded from the study.

Animal disposition: All 40 guinea pigs completed the experiment with no death, exclusion, or withdrawal.

Acquisition, cultivation and identification of neural stem cells

Hippocampal tissues were harvested from newborn guinea pigs and digested with trypsin. The digestion was terminated using a serum-containing medium. The cell suspension was centrifuged at 1000 r/min for 5 minutes and the pellet was collected. The cells were resuspended in complete medium and adjusted to an appropriate density before being seeded into culture flasks. The flasks were incubated in a 37°C, 5% CO_2 incubator. The medium was changed regularly and the cells were passaged when they reached 80–90% confluence. For the experiments, fourth-passage cells were used.

Compound intervention of neural stem cells and grouping

Neural stem cells were divided into a blank control group and a quinazoline-treated group. The control group was treated with PBS, while the treatment groups were exposed to quinazoline at concentrations of 20, 40 and 60 μg/mL, respectively. All cell intervention experiments were independently repeated three times.

Cell proliferation

Cell viability was assessed using the CCK-8 assay (Yang *et al*., 2021); after cell seeding and culture, CCK-8 reagent was added and incubated and absorbance was measured at 450 nm using a microplate reader. Cell proliferation was evaluated using the EdU assay: Cells were incubated with EdU, then fixed and permeabilized, and stained with fluorescent dye according to the kit instructions. Nuclei were counterstained with DAPI and samples were observed under a fluorescence microscope. For all proliferation experiments (CCK-8 and EdU), three replicate wells were set under the upper condition and the experiments were independently repeated three times.

Cell differentiation

The passaged neural stem cells after different treatments were centrifuged and resuspended to adjust the cell density to 1×10^5/L. Afterward, they were inoculated (1mL per well)

and cultured for 5 days. The 30-minute co-staining of DAPI, NSE and GFAP (diluted in 1: 100) was conducted, the results of which were observed under a microscope. Cell differentiation immunofluorescence staining experiment (Wu *et al*., 2025) was independently repeated three times.

Establishment of cisplatin-induced hearing loss model

A guinea pig model of hearing loss was established by intraperitoneal injection of cisplatin, following the method described in the literature (Tzelnick *et al*., 2023). Except for the control group, all guinea pigs in the other groups received intraperitoneal injections of cisplatin (4 mg/kg·d) for six consecutive days. The control group was injected with an equivalent volume of normal saline.

Hearing test

The auditory brainstem response was used to measure hearing. The ABR values were measured before modeling and 1 week later after the transplantation. After anesthetization, the ABR values were measured using an auditory brainstem response instrument with the following parameters: 80-3000Hz as the wave range, 5-97dB as the intensity, 5dB as the interval, 1024 times of superimposition, 10 ms. The ABR threshold measurement for each guinea pig was independently repeated three times and the average value was taken as the final threshold.

Acquisition and morphological observation of cochlear tissues

After anesthetization, the thoracic cavity was opened to expose the thoracic tissue. Then intubate the aorta and perfuse with a proper amount of saline solution, followed by the blood leakage and washing. Afterwards, a one-hour perfusion with PBS solution was conducted. Then the bilateral temporal bones were removed to expose the cochlear tissue, which was then processed to fixation with pentos dialdehyde solution, decalcification using EDTA solution, dehydration, embedment, slice section and HE staining sequentially. Subsequently, cochlear tissues from three randomly selected guinea pigs per group were processed for dehydration, paraffin embedding, sectioning (5 μm thickness) and HE staining for morphological observation.

The morphological evaluation of cochlear tissues was conducted primarily through qualitative observation of HE-stained sections (Dunn *et al*., 2024) under an optical microscope, focusing on the integrity of the cochlear hair cell layer, the arrangement of supporting cells and the morphological structure of the stria vascularis. This study did not perform quantitative morphological analyses, such as hair cell counting or measurement of stria vascularis thickness.

Quantitative real-time PCR(qPCR) quantification of miR-183 expression in cochlear tissues

Total RNA was extracted from the aforementioned cochlear tissues using the TRIzol method and RNA concentration and purity (A260/A280 ratio between 1.8 and 2.0) were determined using NanoDrop. Subsequently, reverse transcription was performed with MicroRNA(miRNA)-specific stem-loop primers to convert miRNA into Complementary DNA(cDNA). qPCR was carried out on a quantitative PCR instrument using the SYBR Green method. The reaction protocol was set as follows: initial denaturation at 95°C for 30 seconds, followed by 40 cycles of denaturation at 95°C for 5 seconds and annealing/extension at 60°C for 30 seconds. Three technical replicates were set up for each sample and the experiment was independently repeated three times as biological replicates. The relative expression of miR-183 was calculated using the $2^{-\Delta\Delta Ct}$ method, normalized to the β-actin snRNA as an internal reference gene. Primer sequences are listed in table 1.

Observation indicators

The following indicators were denoted: the differentiation and proliferation capabilities of neural stem cells, ABR threshold before and after modeling and relative expression of miR-183 in cochlear tissues.

Statistical analysis

SPSS-26.0 and GraphPad Prism software were employed for data analysis. The following data were denoted as ($\bar{x} \pm s$): proliferation rate of neural stem cells, ABR thresholds before and after modeling and relative quantity of miR-183 expression in cochlear tissues. Comparisons of data from three or more groups were performed using the F-test, with either the LSD test (homogeneity of variance test when $P>0.05$) or the Tamhanei test (homogeneity of variance test when $P<0.05$) as the post hoc test. The comparisons within the same group were performed using paired *t*-test. The comparison was considered statistically significant when its *p-value* was less than 0.05. To ensure the reliability of the data, all *in-vitro* cell experiments (proliferation, differentiation, intervention) were independently repeated at least three times.

RESULTS

Identification of neural stem cells

The following positive rates were denoted: Nestin (Fig. 1a) and Sox2 (Fig. 1b) (more than 95%), DAPI (100%) (Fig. 1c), with a double-positive rate of 97.18±1.73% (Fig. 1d).

Compound exerted the pro-differentiation and pro-proliferation effects on neural stem cells

After receiving treatment with different concentrations of the compound, the neural stem cells exhibited a significantly higher OD450 value than those in the blank group ($P<0.05$).

Table 1: Primer sequences.

Genes	Sequence of the primers		Length of primers (bp)
miR-183	Forward	5'-GATCGCTGGTTAAGGCAATTAACAGAG-3'	25
	Reverse	5'-GAACTAGATAGGCGTCATGCTATAGAG-3'	
DNA marker	Forward	5'-GACATGATATGACTTAGAGGGTG-3'	22
	Reverse	5'-GATGATAAGCGAATCTGTCGAAC-3'	

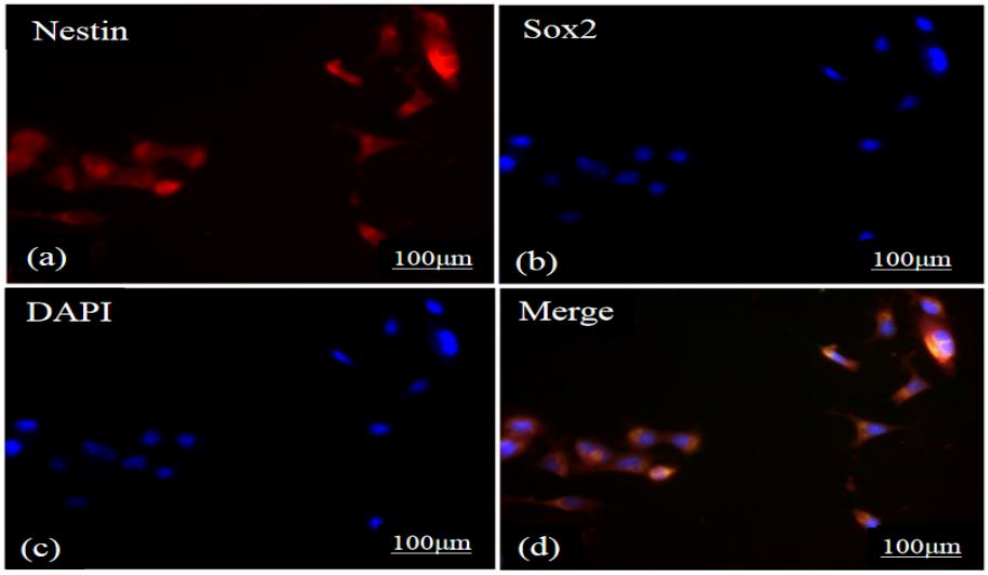

Fig. 1: Immunofluorescence staining of neural stem cell markers. (a) Nestin (green); (b) Sox2 (red); (c) DAPI (blue, nuclear counterstain); (d) Merge of (a), (b) and (c). Scale bar = 100 μm.

Table 2: The proliferation rates of neural stem cells.

Groups	Number of experiments	OD450
Control group	5	0.125±0.013
20μg/ml	5	0.138±0.014*
40μg/ml	5	0.176±0.013*#
60μg/ml	5	0.189±0.015*#
F	-	7.210
P	-	0.000

Note: Compared with the blank group, *P<0.05; compared with the 20μg/mL treatment group, #P<0.05. OD450 refers to the absorbance value at a wavelength of 450 nm (arbitrary units).

Moreover, there was no statistically significant difference in OD450 values between cells treated with 40 μg/mL and 60 μg/mL of the compound (P > 0.05). Therefore, 40 μg/mL of the compound was used in subsequent experiments (Table 2).

Compared to the blank group (0.097±0.006%) (Fig. 2a), the 40μg/mL group had a significantly increased cell proliferation rate (0.157±0.007%) (*P*<0.05, Fig. 2b).

The differentiation potential of cells in the 40μg/mL group was also significantly stronger than that in the blank group (*P*<0.05). There was no significant difference between the 40 μg/mL and 60 μg/mL treatment groups, so a lower concentration was selected to reduce potential toxicity.

Compound ameliorated the inner ear damage through its pro-differentiation and pro-proliferation effects on neural stem cells

Prior to modeling, there was no statistically significant difference in ABR thresholds among the guinea pigs in each group (*P*>0.05). After transplantation, the control group exhibited the lowest threshold, the model group the highest, whereas the transplantation and enhancement groups fell between the two (Table 3). Notably, relative to the blank group (24.23 ± 4.22 dB) (Fig. 3a), the enhancement group (14.61 ± 4.25 dB) had a significantly lower ABR threshold (*P*<0.05, Fig. 3b).

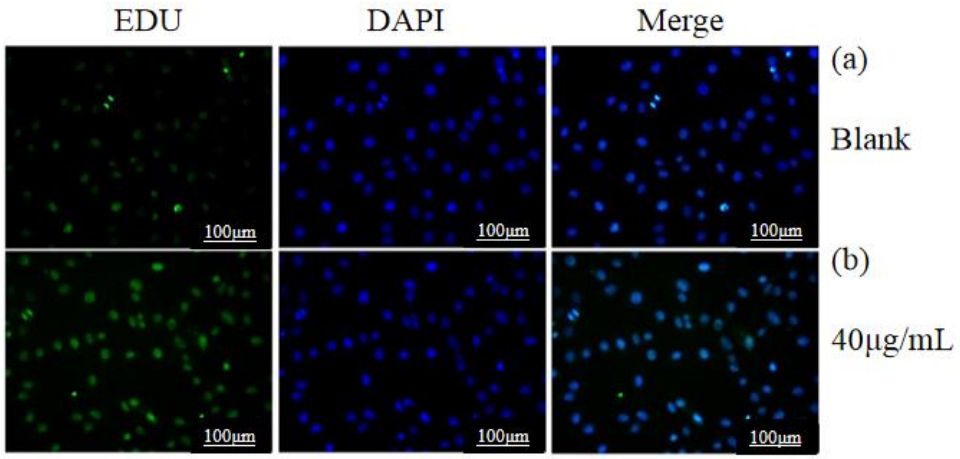

Fig. 2 Effect of quinazoline on neural stem cell proliferation assessed by EdU incorporation assay. EdU-positive cells (green) represent proliferating cells; DAPI (blue) stains all nuclei. (a) Control group: NSCs treated with PBS (vehicle control) showing baseline proliferation; (b) Quinazoline treatment group: NSCs treated with 40 μg/mL quinazoline showing increased number of EdU-positive cells compared to control. Quantification confirmed that quinazoline significantly enhanced NSC proliferation rate (P<0.05). Scale bar = 100 μm (applies to both panels).

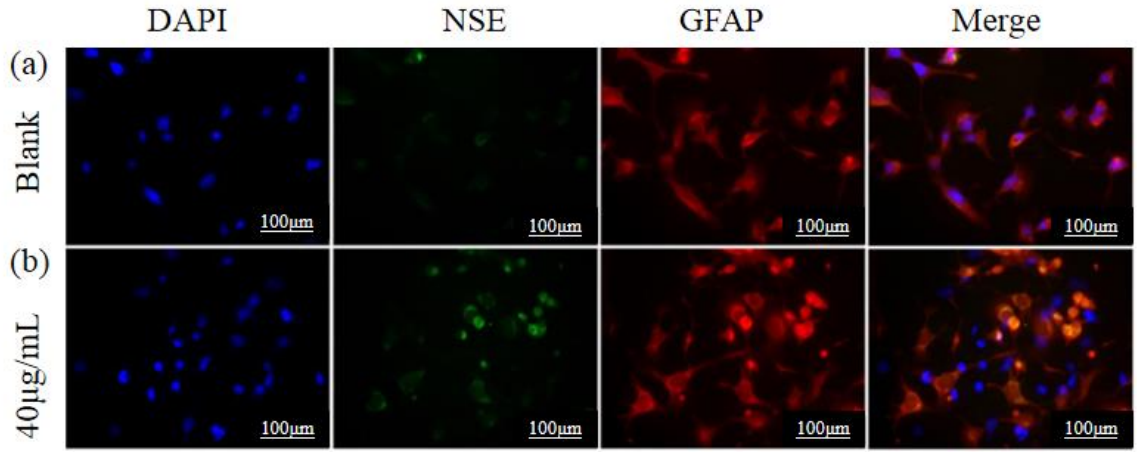

Fig. 3 Effect of quinazoline on neural stem cell differentiation assessed by immunofluorescence staining of neuronal and glial markers. Green: NSE (neuron-specific enolase, a neuronal marker). Red: GFAP (glial fibrillary acidic protein, an astrocyte marker). Blue: DAPI (nuclear counterstain). (a) Control group (PBS treatment): NSCs differentiated under standard conditions showing baseline levels of NSE and GFAP expression; (b) Quinazoline treatment group (40 μg/mL): NSCs pretreated with quinazoline showed significantly increased expression of both NSE and GFAP compared to control, indicating enhanced differentiation into both neuronal and glial lineages. Scale bar = 100 μm (applies to both panels).

Table 3: Difference analysis of ABR thresholds (2 pairs of inner ears) ($\bar{x} \pm s$,dB).

Groups	Number of experiments	Before modeling	After transplantation	Paired t-test	*P*
Control group	5	4.50±3.55	4.50±3.35	0.000	1.000
Model group	5	4.45±3.75	64.47±3.73*	25.374	0.000
Transplantation group	5	4.25±4.21	24.23±4.22*#	7.495	0.000
Enhancement group	5	4.65±4.20	14.61±4.25*#&	3.727	0.006
F	-	0.022	26.747	-	
P	-	0.983	0.000	-	

Note: Compared with the control group, *P<0.05; compared with the model group, #P<0.05; compared with the transplantation group, and P<0.05. Quantification of functional recovery: The difference in threshold between the transplantation group and the model group is approximately 40.2 dB. The difference in thresholds between the enhancement group and the model group was approximately 49.9 dB. The enhanced group recovered an additional approximately 9.7 dB compared to the transplantation group.

Qualitative morphological observations revealed that the cochlear structure of guinea pigs in the control group was clear, with normal morphology of the stria vascularis (Fig. 4a). In contrast, the cochlear tissues of the model group displayed disorganized cell arrangement along with marked dilation of the stria vascularis (Fig. 4b). In the transplantation group, the damaged cochlear tissues showed improvement, with more orderly cell arrangement and gradual restoration of the stria vascularis morphology (Fig. 4c), which was even more pronounced in the enhancement group (Fig. 4d).

Amelioration of the inner ear damage by compound may involve the up-regulated miR-183 and its pro-differentiation and pro-proliferation effects on neural stem cells

PCR results showed that after normalization with β-actin, the relative expression of miR-183 was lowest in the model group, followed by the control group, transplantation group and enhancement group. Specifically, compared with the control group, miR-183 expression in the model group was down-regulated to approximately 0.36-fold; in the transplantation group, it recovered to about 1.41-fold of the control level; while in the enhancement group, it was further up-regulated to about 1.87-fold of the control level. Notably, miR-183 expression in the enhancement group was significantly higher than that in the transplantation group (approximately 1.33-fold, $P<0.05$). (Table 4 and Fig. 5).

DISCUSSION

This study aimed to investigate whether the compound can alleviate inner-ear damage by enhancing the proliferation and differentiation potential of neural stem cells. Neural stem cells isolated from newborn guinea pigs were either pretreated with quinazoline or left untreated before transplantation into guinea pigs with inner ear damage. Using this model, the current study examined the effects of compound-enhanced neural stem cells on inner-ear damage. The cisplatin-induced hearing loss model was established using guinea pigs. Compared with the healthy control group, guinea pigs in the model group exhibited a significantly higher ABR threshold. The observation of disordered cell arrangement and an expanded stria vascularis in the model group, compared to the clear structure in controls, indicated the successful establishment of the cisplatin-induced hearing-loss model. The cochlear tissues of guinea pigs in the model group displayed disorderly arranged cells, which were accompanied by an obviously expanded stria vascularis. Nonetheless, the cochlear tissues in the control group exhibited a clear structure without any abnormality in the morphology of stria vascularis. It indicated the successful establishment of the cisplatin-induced hearing-loss model, which can be used in subsequent experiments. In addition, we also identified the harvested neural stem cells from newborn guinea pigs using several specific markers. The following positive rates were denoted: DAPI (100%), Nestin and Sox2 (more than 95%), with a double-positive rate of 97.18±1.73%. It indicated a successful acquisition of the neural stem cells from newborn guinea pigs and these cells can be utilized for subsequent experiments.

In order to determine the optimal concentration of compound for neural stem cell intervention, 20μg/mL, 40μg/mL and 60μg/mL of compound concentrations were investigated in the current study. The results showed that increasing the quinazoline concentration led to stronger proliferation in neural stem cells. However, since no significant difference in proliferation was observed between the 40 μg/mL and 60 μg/mL treatments, the lower concentration (40 μg/mL) was selected for subsequent experiments to minimize potential toxicity. Consistent with this, the 40 μg/mL quinazoline treatment group showed significantly improved proliferation and differentiation capabilities compared to the blank control, indicating that quinazoline can effectively enhance NSC function (Joshi *et al*., 2021).

Further experiments were conducted to analyze the amelioration differences between compound-enhanced and unenhanced neural stem cells in inner ear damage, which was assessed by measuring ABR thresholds and changes in cochlear morphology in guinea pigs. The results showed no statistically significant difference in ABR thresholds among guinea pigs before modeling. After transplantation, the lowest ABR threshold was observed in the control group, while the highest ABR threshold was observed in the model group, followed by those in the transplantation group and the enhancement group. Furthermore, the ABR threshold in the enhancement group was significantly lower than that in the transplantation group. A reduction of approximately 10 dB in the ABR threshold typically corresponds to a doubling of auditory sensitivity to sound intensity for functional perception. This indicates that, compared to untreated neural stem cells, transplantation of quinazoline-pretreated cells more effectively promotes the recovery of electrophysiological function in the auditory pathway. In combination with the ABR results, the observed restoration of a more favorable environment for supporting cells and hair cells and more organized stria vascularis structure likely provides a direct anatomical basis for the lower ABR thresholds. This suggests that quinazoline pretreatment enhances the reparative potential of NSCs, thereby facilitating coordinated recovery of cochlear microstructure and macro-function. From the perspective of functional recovery magnitude, compared to the fully impaired model group, transplantation of untreated NSCs (transplantation group) restored the ABR threshold by an average of approximately 40.2 dB, while transplantation of quinazoline-pretreated NSCs (enhancement group) restored it by about 49.9 dB—an improvement of nearly 10 dB.

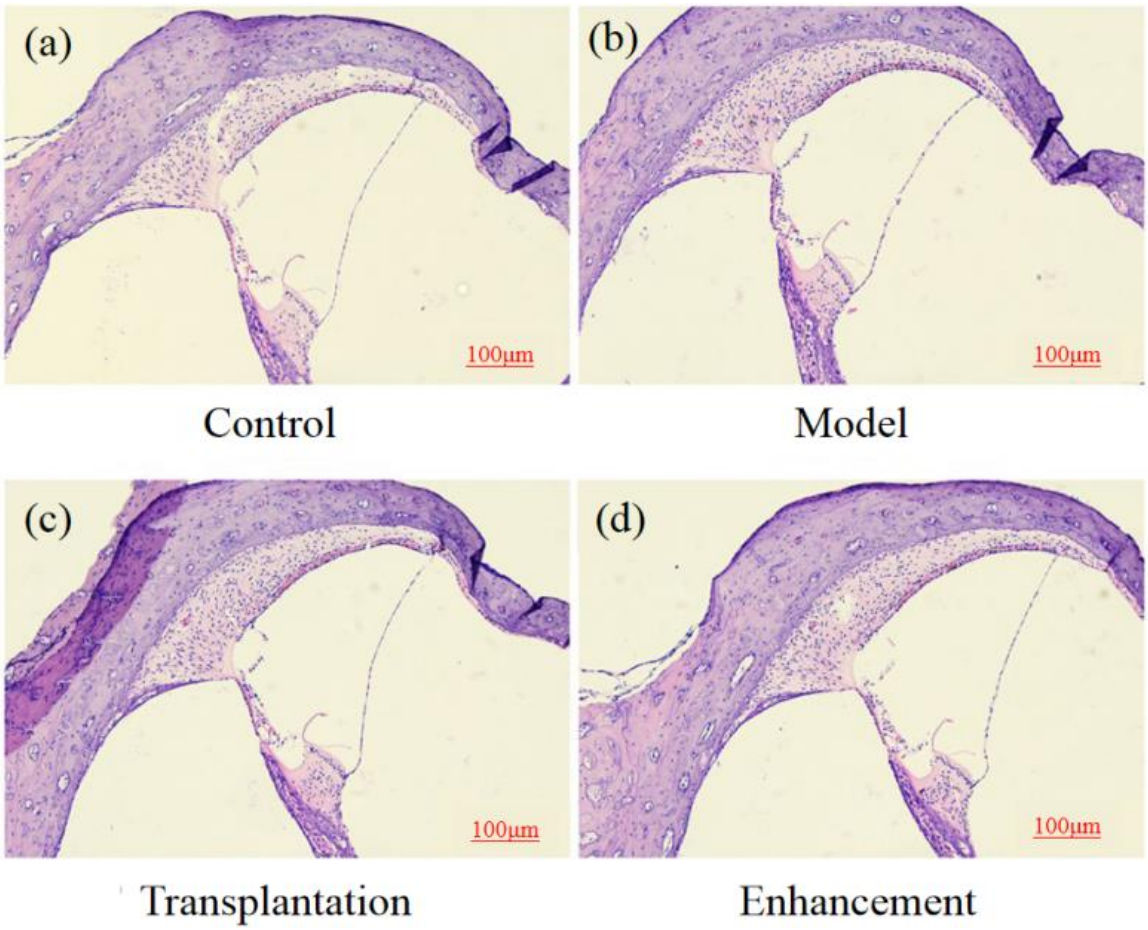

Fig. 4 Representative HE-stained sections of guinea pig cochlear tissues from each experimental group. Sections show the organ of Corti and stria vascularis morphology. (a) Control group (healthy guinea pigs): clear cochlear structure with normal, well-organized cell arrangement and intact stria vascularis; (b) Model group (cisplatin-induced hearing loss, no treatment): disorganized cell arrangement, loss of hair cell layer integrity and marked dilation (swelling) of the stria vascularis; (c) Transplantation group (cisplatin + untreated NSC transplantation): partial improvement in cell arrangement and moderate restoration of stria vascularis morphology compared to model group; (d) Enhancement group (cisplatin + quinazoline-pretreated NSC transplantation): most pronounced structural restoration, with well-organized cell layers and near-normal stria vascularis morphology. Scale bar = 100 μm (applies to all panels). Abbreviations: HE, hematoxylin and eosin; NSC, neural stem cell.

Table 4: Relative expression of miR-183 (normalized to β-actin, $\bar{x} \pm s$).

Groups	Number of experiments	miR-183/β-actin
Control group	5	0.105±0.012
Model group	5	0.038±0.011*
Transplantation group	5	0.148±0.014*#
Enhancement group	5	0.196±0.015*#
F	-	18.993
P	-	0.000

Note: The expression level of miR-183 was calculated using the 2^−Δ ΔCt^ method and was expressed as the ratio relative to the reference gene β-actin (without units, it is a relative quantitative value).t

In audiology, a 10 dB difference generally corresponds to approximately a doubling of auditory sensitivity to sound intensity, indicating that quinazoline pretreatment yields a functionally meaningful biological gain. Therefore, quinazoline pretreatment is not only an effective adjuvant approach but also a therapeutic strategy that delivers substantial functional benefits. Moreover, this ameliorating effect on inner ear damage can be further enhanced by the compound, leading to greater improvement in hearing function in guinea pigs.

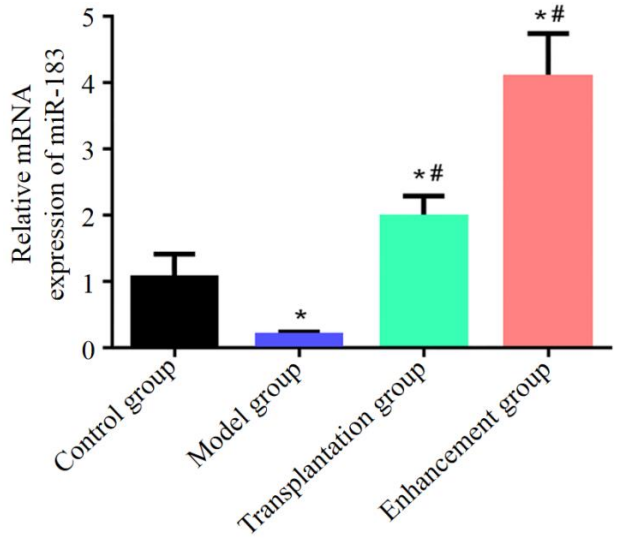

Fig. 5: Agarose gel electrophoresis of qPCR products showing miR-183 expression in cochlear tissues of each experimental group. Lanes 1-4: miR-183 amplicons. Lanes 2, 4, 6, 8: β-actin (internal control) amplicons. Lane 1 (Control group): moderate miR-183 expression. Lane 2 (Model group): markedly reduced miR-183 expression (approximately 0.36-fold of control). Lane 3 (Transplantation group): recovered miR-183 expression (approximately 1.41-fold of control). Lane 4 (Enhancement group): highest miR-183 expression (approximately 1.87-fold of control). β-actin bands show equal loading across all samples. M = DNA molecular weight marker (sizes in base pairs, bp). Relative expression was calculated using the 2^−ΔΔCt^ method normalized to β-actin. Abbreviations: qPCR, quantitative real-time polymerase chain reaction.

Additionally, the morphology of cochlea tissues was also under observation, which indicated more significant morphological improvement in the enhancement group compared to the transplantation group. This improvement may be attributed to the quinazoline-induced enhancement of NSC proliferation and differentiation. These enhanced NSCs could potentially mitigate tissue edema and hair cell permeability, thereby alleviating hypoxia and promoting hair cell survival, which collectively contribute to the amelioration of inner ear damage and hearing recovery (Lakshman *et al*., 2021). This study mainly focused on the hearing function and structural changes of guinea pigs to demonstrate that this compound can exert its protective effects on the inner ear damage of guinea pigs, but its specific mechanism remains to be studied.

Generally, miRNA specifically binds to its related target genes, thereby modulating the expression of these target genes (Langhnoja *et al*., 2021). Studies have revealed that the miR-183 family can affect the function and development of nerves and can also protect against neurosensory destructive stimulation (Li *et al*., 2021a). In addition, another study (Li *et al*., 2021b) found that miR-183 expression was elevated in inner ear tissues and was associated with hair cell viability. Therefore, the expression changes of miR-183 following inner ear damage have attracted increasing attention from researchers in recent years. The current study disclosed that the relative quantity of miR-183 expression was the lowest in the model group, followed by the control group, transplantation group and enhancement group. In particular, significantly higher miR-183 expression was observed in the enhancement group compared with the transplantation group. It is noteworthy that the upregulation of miR-183 expression showed a clear correlation with morphological improvement in cochlear tissues.

In the enhancement group, which exhibited the most significant morphological restoration, miR-183 expression was also the highest. Previous studies have confirmed that members of the miR-183 family play critical roles in the development, survival and functional maintenance of auditory hair cells and downregulation of their expression is closely associated with hair cell apoptosis and hearing loss (Krohs *et al*., 2021). Therefore, the observed upregulation of miR-183 in this study likely directly contributed to the more organized cellular arrangement and restored stria vascularis morphology in the enhancement group. Specifically, miR-183 may promote the differentiation of supporting cells into hair cell-like phenotypes by inhibiting target genes such as Sox2 and PAX6 (Davari *et al*., 2023) or enhance the stability of hair cells and their supporting structures by regulating cell cycle and apoptosis-related pathways, thereby achieving more effective structural repair. Given that miR-183 is a key regulatory factor for auditory hair cell survival (Krohs *et al*., 2021), its coordinated upregulation in the enhancement group strongly suggests that quinazoline pretreatment may enhance the protective effects of transplanted NSCs on hair cells or promote endogenous repair by upregulating miR-183 expression in the inner ear microenvironment. This could be one of the key molecular events underlying the superior functional recovery and structural restoration observed.

Although this study demonstrates that quinazoline pretreatment can effectively enhance the therapeutic potential of neural stem cells by upregulating miR-183, thereby improving inner ear structure and function, several limitations remain. The animal sample size in this experiment was relatively small, which may affect statistical power. Furthermore, when selecting the optimal drug concentration, dose-dependent effects beyond 60 μg/mL were not tested, potentially limiting the scope of the findings. Additionally, the efficacy was validated only in a single cisplatin-induced hearing loss model in guinea pigs; whether the conclusions apply to inner ear injuries from other etiologies or in other species requires further investigation. Moreover, the mechanistic investigation primarily focused on changes in miR-183 expression.

While the findings suggest a potential role, causality has not been directly verified through gain- or loss-of-function experiments, nor have downstream target genes and the specific signaling pathways involved been thoroughly explored. Therefore, the complete molecular mechanism by which quinazoline promotes the repair of inner ear injury by neural stem cells remains to be systematically elucidated.

CONCLUSION

In summary, the quinazoline exerted significant pro-differentiation and pro-proliferation effects on neural stem cells. The quinazoline-enhanced and unenhanced neural stem cells were then transplanted into guinea pigs with inner-ear damage. The quinazoline-enhanced neural stem cells can significantly improve hearing in guinea pigs and lower the ABR threshold. Its major mechanism involves the upregulation of miR-183 in the cochlear tissues. Nevertheless, a certain limitation also exists in this study. It requires further exploration of the mechanisms by which quinazoline enhances neural stem cell differentiation and proliferation to alleviate inner ear damage. Moreover, this study reported, for the first time, that its mechanism involves upregulated miR-183, whose specific target genes require further elucidation.

Acknowledgments
We gratefully acknowledge Shanxi Children's Hospital and Shanxi Maternal and Child Health Hospital for providing the necessary equipment for this study.

Authors' contributions
Qinxue Wang: Experimental design, data collection and analysis, manuscript writing, research guidance, manuscript revision and review; Yin Wang: Experimental operation, data processing, material provision and technical support. All authors have read and agreed to the final manuscript.

Funding
There was no funding.

Ethical approval
This study was approved by the ethics committee of Shanxi Maternal and Child Health Hospital (No. SMCHH-E-22-03-04). This study was performed in adherence with the ARRIVE guidelines. See supplementary file for the ARRIVE checklist.

Data availability statement
The datasets generated and/or analyzed during the current study period are available from the corresponding authors upon reasonable request.

Conflicts of interest
The author states that this research was conducted without any commercial or financial interests that could be interpreted as potential conflicts of interest. There are no conflicts to declare.

Supplementary data

REFERENCES

Chao KY, Huang WY, Ho CY, Wan D, Wang HC, Yang CY and Wang TW (2021). Biodegradable aniline-derived electroconductive film for the regulation of neural stem cell fate. *J Mater Chem B*., **9**(5): 1325-1335.

Chen D, Liu J, Wu Z and Li SH (2021). Role of miR-132/methyl-CpG-binding protein 2 in the regulation of neural stem cell differentiation. *Neural Regen Res*., **16**(2): 345-349.

Cui Y, Yin Y, Zou Y, Zhao Y, Han J, Xu B, Chen B, Xiao Z, Song H, Shi Y, Xue W, Ma X and Dai J (2021). The rotary cell culture system increases NTRK3 expression and promotes neuronal differentiation and migratory ability of neural stem cells cultured on collagen sponge. *Stem Cell Res Ther.,* **12**(1): 298.

Davari M, Soheili ZS, Latifi-Navid H and Samiee S (2023). Potential involvement of miR-183/96/182 cluster-gene target interactions in transdifferentiation of human retinal pigment epithelial cells into retinal neurons. *Biochem Biophys Res Commun*., **663**: 87-95.

Diener J and Sommer L (2021). Reemergence of neural crest stem cell-like states in melanoma during disease progression and treatment. *Stem Cells Transl Med*., **10**(4): 522-533.

Dong Q, Zavortink M, Froldi F, Golenkina S, Lam T and Cheng LY (2021). Glial Hedgehog signalling and lipid metabolism regulate neural stem cell proliferation in Drosophila. *EMBO Rep*., **22**(5): e52130.

Dray N, Than-Trong E and Bally-Cuif L (2021). Neural stem cell pools in the vertebrate adult brain: Homeostasis from cell-autonomous decisions or community rules? *Bioessays*., **43**(3): e2000228.

Durán Alonso MB (2026). Autophagy in Sensorineural Hearing Loss: Jekyll or Hyde?. *Int J Mol Sci*., **27**(4):2053.

Dunn C, Brettle D, Cockroft M, Keating E, Revie C and Treanor D (2024). Quantitative assessment of H and E staining for pathology: Development and clinical evaluation of a novel system. *Diagn Pathol*., **19**(1): 42.

Gastfriend BD, Stebbins MJ, Du F, Shusta EV and Palecek SP (2021). Differentiation of brain pericyte-like cells from human pluripotent stem cell-derived neural crest. *Curr Protoc*., **1**(1): e21.

Gao M, Dong Q, Wang W, Yang Z, Guo L, Lu Y, Ding B, Chen L, Zhang J and Xu R (2021). Induced neural stem cell grafts exert neuroprotection through an interaction between Crry and Akt in a mouse model of closed head injury. *Stem Cell Res Ther*., **12**(1): 128.

Gong Y, Duan H, Wang X, Zhao C, Li W, Dong C, Li Z and Zhou Q (2021). Transplantation of human induced

pluripotent stem cell-derived neural crest cells for corneal endothelial regeneration. *Stem Cell Res Ther*., **12**(1): 214.

Haag D, Mack N, Benites Goncalves da Silva P, Statz B, Clark J, Tanabe K, Sharma T, Jager N, Jones DTW, Kawauchi D, Wernig M and Pfister SM (2021). H3.3-K27M drives neural stem cell-specific gliomagenesis in a human iPSC-derived model. *Cancer Cell*., **39**(3): 407-422 e413.

Han MJ, Lee WJ, Choi J, Hong YJ, Uhm SJ, Choi Y and Do JT (2021). Inhibition of neural stem cell aging through the transient induction of reprogramming factors. *J Comp Neurol*., **529**(3): 595-604.

Hayashi K, Suzuki Y, Fujimoto C and Kanzaki S (2020). Molecular mechanisms and biological functions of autophagy for genetics of hearing impairment. *Genes (Basel),* **11**(11): 1331.

Hirai T, Kono K, Sawada R, Kuroda T, Yasuda S, Matsuyama S, Matsuyama A, Koizumi N, Utoguchi N, Mizuguchi H and Sato Y (2021). A selective cytotoxic adenovirus vector for concentration of pluripotent stem cells in human pluripotent stem cell-derived neural progenitor cells. *Sci Rep*., **11**(1): 11407.

Huang D, Cao Y, Yang X, Liu Y, Zhang Y, Li C, Chen G and Wang Q (2021). A nanoformulation-mediated multifunctional stem cell therapy with improved beta-amyloid clearance and neural regeneration for Alzheimer's disease. *Adv Mater*., **33**(13): e2006357.

Jia G, Diao Z, Liu Y, Sun C and Wang C (2021). Neural stem cell-conditioned medium ameliorates a beta25-35-induced damage in SH-SY5Y cells by protecting mitochondrial function. *Bosn J Basic Med Sci*., **21**(2): 179-186.

Joshi BS and Zuhorn IS (2021). Heparan sulfate proteoglycan-mediated dynamin-dependent transport of neural stem cell exosomes in an *in-vitro* blood-brain barrier model. *Eur J Neurosci*., **53**(3): 706-719.

Krohs C, Korber C, Ebbers L, Altaf F, Hollje G, Hoppe S, Dorflinger Y, Prosser HM and Nothwang HG (2021). Loss of miR-183/96 alters synaptic strength via presynaptic and postsynaptic mechanisms at a central synapse. *J Neurosci*., **41**(32): 6796–6811.

Lakshman N, Bourget C, Siu R, Bamm VV, Xu W, Harauz G and Morshead CM (2021). Niche-dependent inhibition of neural stem cell proliferation and oligodendrogenesis is mediated by the presence of myelin basic protein. *Stem Cells*., **39**(6): 776-786.

Langhnoja J, Buch L and Pillai P (2021). Potential role of NGF, BDNF and their receptors in oligodendrocytes differentiation from neural stem cell: An *in-vitro* study. *Cell Biol Int*., **45**(2): 432-446.

Li W, Zhao Z, Lu Z, Ruan W, Yang M and Wang D (2022). The prevalence and global burden of hearing loss in 204 countries and territories, 1990-2019. *Environ Sci Pollut Res Int.,* **29**(8): 12009-12016.

Li G, Zhang B, Sun JH, Shi LY, Huang MY, Huang LJ, Lin ZJ, Lin QY, Lai BQ, Ma YH, Jiang B, Ding Y, Zhang HB, Li MX, Zhu P, Wang YQ, Zeng X and Zeng YS (2021a). An NT-3-releasing bioscaffold supports the formation of TrkC-modified neural stem cell-derived neural network tissue with efficacy in repairing spinal cord injury. *Bioact Mater.,* **6**(11): 3766-3781.

Li X, Gao Y, Tian F, Du R, Yuan Y, Li P, Liu F and Wang C (2021b). miR-31 promotes neural stem cell proliferation and restores motor function after spinal cord injury. *Exp Biol Med (Maywood)*., **246**(11): 1274-1286.

Tzelnick S, Mizrachi A, Barkan N, Shivatzki S, Yosefof E, Hikri E, Attias J and Hilly O (2023). The protective effect of aspirin-induced temporary threshold shift in an animal model of cisplatin-related ototoxicity. *J Cancer Res Clin Oncol.,* **149**(5): 2009-2016.

Wu E, Bieniosek M, Wu Z, Thakkar N, Charville GW, Makky A, Schürch CM, Huyghe JR, Peters U, Li C I, Li L, Giba H, Behera V, Raman A, Trevino AE, Mayer AT and Zou J (2025). ROSIE: AI generation of multiplex immunofluorescence staining from histopathology images. *Nat Commun*., **16**(1): 7633.

Yang X, Zhong Y, Wang D and Lu Z (2021). A simple colorimetric method for viable bacteria detection based on cell counting Kit-8. *Anal Methods*., **13**(43): 5211–5215.